Nematicity Arising from a Chiral Superconducting Ground State in Magic-Angle Twisted Bilayer Graphene under In-Plane Magnetic Fields

Tao Yu,[1] Dante M. Kennes,[2,1] Angel Rubio,[1,3,4] and Michael A. Sentef[1]

[1] *Max Planck Institute for the Structure and Dynamics of Matter, Luruper Chaussee 149, 22761 Hamburg, Germany*
[2] *Institut für Theorie der Statistischen Physik, RWTH Aachen University and JARA-Fundamentals of Future Information Technology, 52056 Aachen, Germany*
[3] *Center for Computational Quantum Physics (CCQ), The Flatiron Institute, 162 Fifth Avenue, New York, New York 10010, USA*
[4] *Nano-Bio Spectroscopy Group, Departamento de Física de Materiales, Universidad del País Vasco, 20018 San Sebastian, Spain*

(Dated: January 6, 2021)

Recent measurements of the resistivity in magic-angle twisted bilayer graphene near the superconducting transition temperature show two-fold anisotropy, or nematicity, when changing the direction of an in-plane magnetic field [Cao *et al.*, arXiv:2004.04148]. This was interpreted as strong evidence for exotic nematic superconductivity instead of the widely proposed chiral superconductivity. Counter-intuitively, we demonstrate that in two-dimensional chiral superconductors the in-plane magnetic field can hybridize the two chiral superconducting order parameters to induce a phase that shows nematicity in the transport response. Its paraconductivity is modulated as $\cos(2\theta_{\mathbf{B}})$, with $\theta_{\mathbf{B}}$ being the direction of the in-plane magnetic field, consistent with experiment in twisted bilayer graphene. We therefore suggest that, surprisingly, the nematic response reported by Cao *et al.* could provide experimental support for, rather than against, a chiral superconducting state.

Introduction.—Knowledge of the pairing symmetry is key in understanding the behavior of superconductors as well as for various applications thereof. These pairing symmetries are fundamental properties of the superconducting state and yield robust insights even irrespective of the details of the underlying microscopic pairing mechanisms [1–3]. The recently discovered superconducting phase close to the correlated insulating phase in magic-angle twisted bilayer graphene (MATBG) [4–7] has spurred tremendous research activities. However, the pairing symmetry of the superconducting state has not been identified experimentally. Pairing mechanisms based on phonons [8–13] or pure Coulomb interaction [14–32] have been proposed, among which the pure electronic origins often favor the chiral $(d \pm id)$-wave superconductivity with promising applications in topological quantum computing. Chiral $(d \pm id)$-wave superconductivity retains the rotational symmetry but breaks the time-reversal one, by mechanism similar to the one previously studied in heavily doped single layer graphene [33, 34]. The existing evidence for chiral superconductivity in other materials, such as UPt_3 [35–37] and UTe_2 [38], has so far not been reported in MATBG.

Recent transport measurements in MATBG provided key features of the pairing symmetry of the superconducting state by revealing a two-fold anisotropy or nematicity in the resistivity around the superconducting transition temperature T_c when changing the direction of a relatively-strong ($\gtrsim 0.5$ T) in-plane magnetic field [39]. The transport response is still isotropic when the magnetic field is smaller. At first glance it appears that chiral superconductivity should be ruled out since it respects the three-fold rotation symmetry of the lattice. Nematic superconductivity—an exotic phase that breaks the lattice rotational symmetry but respects the translational one—may be favored, which was phenomenologically proposed to be a complicated coexisting phase [40] or intrinsic correlated phase [41]. Nematic fluctuation in the correlated insulating phases was indeed observed in MATBG by scanning tunneling microscopy (STM) [42–44], also in twisted double bilayer graphene [45]. But it is not very clear whether the insulating correlated phase is directly related to, or purely competitive with, the superconducting one, in that superconductivity can survive even when the insulating state is completely suppressed [46]. Less attention was, however, paid to the possible role of the in-plane magnetic field for superconductivity. As one marked exception, it was proposed to provide a vector potential to induce the Z_2 symmetry-breaking phase transition in Sr_2RuO_4 films of $(p \pm ip)$-wave chiral superconductors [47]. However, this was not observed since Sr_2RuO_4 may not be a p-wave superconductor, as suggested by recent investigations [48–50].

In this Letter, we formulate the phase transition of a chiral $(d \pm id)$-wave superconductor driven by a critical in-plane magnetic field in a prototype honeycomb lattice of MATBG and demonstrate that the new phase is nematic with two-fold anisotropy in the transport response. We predict an emerging anomalous Hall effect [51] in the paraconductivity of the driven nematic phase, also with a two-fold anisotropy with respect to the direction of the in-plane magnetic field. In detail, the two degenerate chiral states, represented by ξ_1 and ξ_2 at the north and south poles of the Bloch sphere de-

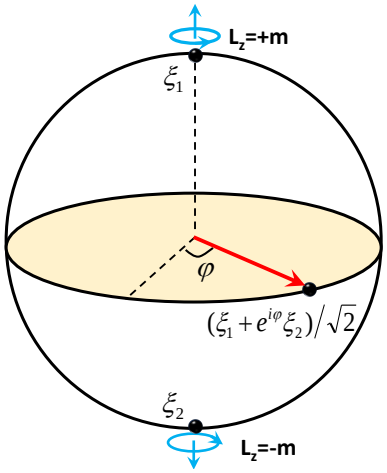

FIG. 1. Hybridization of two degenerate chiral states on the Bloch sphere by in-plane magnetic field. Assuming the north and south poles represent two chiral states ξ_1 and ξ_2 with positive and negative angular momentum $+m$ and $-m$, the points on the Bloch sphere represent their superpositions. The in-plane magnetic field can drive the system to be a state $(\xi_1+\exp(i\varphi)\xi_2)/\sqrt{2}$ with equal contributions from the two chiral states, represented by points at the equator and modulated by $\varphi = 2\theta_{\mathbf{B}} + \phi$ via the field direction $\theta_{\mathbf{B}}$ and an irrelevant phase ϕ.

picted in Fig. 1, are coupled via the vector potential of the magnetic field through angular-momentum conservation. When the magnetic field B is larger than a critical one B_c, the two chiral states are hybridized with equal contributions of the form $[\xi_1 + \exp(2i\theta_{\mathbf{B}} + i\phi)\xi_2]/\sqrt{2}$, as depicted by points at the equator of the Bloch sphere. The coefficient of this superposition is modulated by the direction of the magnetic field denoted by angle $\theta_{\mathbf{B}}$ and an irrelevant phase ϕ. Near the superconducting transition temperature T_c the critical field driving the transition becomes arbitrarily small $B_c \to 0$ as $T \to T_c$ (e.g., $B_c \sim 0.6$ T when $T \sim 0.9T_c$). Although the chiral states ξ_1 and ξ_2 are both isotropic, the driven state given by their superposition is nematic with an anisotropy axis modulated by $\cos(2\theta_{\mathbf{B}})$, i.e., showing two-fold nematic response with respect to the applied field. The consistence with experimental measurements [39] indicates that, surprisingly, chiral superconductivity might be supported rather than ruled out in MATBG by these experimental findings. We propose that magnetoelectric transport measurements are useful tools also for other possible $(p \pm ip)$-wave chiral superconductors, such as UPt_3 [35–37] and UTe_2 [38] thin films, to engineer and identify the pairing symmetry.

Effective Ginzburg-Landau Lagrangian.—The microscopic mechanism of superconductivity in MATBG may be sensitive to the detailed structure of the flat bands and many-body interaction as well as electron-phonon coupling [8–32]. Our theory is largely independent of these details by relying solely on the system's symmetry within a Ginzburg-Landau (GL) phenomenology [1]. To be specific for the estimation of material parameters, here we consider the tight-binding model on the honeycomb lattice with two p-orbitals $\{p_x, p_y\}$ on every site proposed by Yuan and Fu [52]. Note, however, that our general conclusions rely on the pairing symmetry of the superconducting state only and are thus applicable beyond this specific microscopic model. The chiral basis is denoted by $(\hat{a}_{\mathbf{k}\pm,\sigma}, \hat{b}_{\mathbf{k}\pm,\sigma})^T = (\hat{a}_{\mathbf{k}x,\sigma} \pm \hat{a}_{\mathbf{k}y,\sigma}, \hat{b}_{\mathbf{k}x,\sigma} \pm \hat{b}_{\mathbf{k}y,\sigma})^T/\sqrt{2}$ on the "A" and "B" sites with $\sigma = \{\uparrow,\downarrow\} = \{+,-\}$ being the electron spin, the Hamiltonian in momentum space is divided into subspaces, given by

$$h_{\pm,\sigma}(\mathbf{k}) = -\mu + t_2(g_{\mathbf{k}} + g_{-\mathbf{k}}) \pm it_3(g_{-\mathbf{k}} - g_{\mathbf{k}}) + \frac{\sigma}{2}g\mu_B B + \begin{pmatrix} 0 & t_1 f_{\mathbf{k}} \\ t_1 f_{-\mathbf{k}} & 0, \end{pmatrix}. \quad (1)$$

Here, μ is the chemical potential; t_1 and $\{t_2, t_3\}$ are the hopping parameters between nearest and fifth neighboring sites that are connected by $\mathbf{c}_{\mu=\{1,2,3\}}$ and $\mathbf{d}_{\mu=\{1,2,3\}}$, respectively [52]; $f(\mathbf{k}) = \sum_{\mu=1,2,3} e^{i\mathbf{k}\cdot\mathbf{c}_\mu}$ and $g(\mathbf{k}) = \sum_{\mu=1,2,3} e^{i\mathbf{k}\cdot\mathbf{d}_\mu}$; and $g\mu_B B$ is the Zeeman splitting via the in-plane magnetic field $\mathbf{B}$. The concrete microscopic mechanism that induces superconductivity is still unclear and is under intensive investigation. Therefore, here we solely rely on the pairing interaction in momentum space that allows to stabilize d-wave superconductivity [1, 30, 53]. The Pauli paramagnetic limit of superconductivity in MATBG [4, 39] suggests a spin-singlet pairing, so we look into the interaction Hamiltonian of the form

$$\hat{H}_{\text{int}} \simeq \sum_{\alpha=\pm}\sum_{\mathbf{k}\mathbf{k}'} V_\alpha(\mathbf{k}-\mathbf{k}')\left(\hat{a}^\dagger_{\mathbf{k}\alpha,\uparrow}\hat{b}^\dagger_{-\mathbf{k}\alpha,\downarrow} - \hat{a}^\dagger_{\mathbf{k}\alpha,\downarrow}\hat{b}^\dagger_{-\mathbf{k}\alpha,\uparrow}\right) \times \left(\hat{b}_{-\mathbf{k}'\alpha,\downarrow}\hat{a}_{\mathbf{k}'\alpha,\uparrow} - \hat{b}_{-\mathbf{k}'\alpha,\uparrow}\hat{a}_{\mathbf{k}'\alpha,\downarrow}\right), \quad (2)$$

where $V_\alpha(\mathbf{k}-\mathbf{k}')$ is the pairing potential that can be decomposed by the irreducible representation of the system's symmetry group D_{6h} [1]. Following the case of heavily doped graphene [30, 33, 34], we employ a rotationally invariant pairing potential of the form

$$V_\alpha(\mathbf{k}-\mathbf{k}') = \frac{V_\alpha}{N}\sum_{\mu=\{1,2,3\}} e^{i(\mathbf{k}-\mathbf{k}')\cdot\tilde{\mathbf{c}}_\mu},$$

where N is the number of honeycomb lattice sites, and the coupling constant $V_\alpha < 0$ and $\tilde{\mathbf{c}}_\mu \parallel \mathbf{c}_\mu$ need to be determined from experimental input.

The effective Lagrangian is described by a bosonic field with multiple components $\vec{\Phi} = (\phi_1, \phi_2, \phi_3)^T$ [54] (see Supplemental Material [55] for details),

$$L_{\text{eff}}[\overline{\phi}, \phi] = \sum_{\mu\mu'=\{1,2,3\}} \int d\mathbf{r}\overline{\phi}_\mu(\mathbf{r},\tau)\mathcal{M}_{\mu\mu'}\phi_{\mu'}(\mathbf{r},\tau) + \sum_{\mu\mu'}\sum_{\delta\gamma=x,y} \mathcal{T}^{\mu\mu'}_{\delta\gamma}\int d\mathbf{r}\partial_\delta\phi^*_\mu(\mathbf{r},\tau)\partial_\gamma\phi_{\mu'}(\mathbf{r},\tau) + O(\phi^4), \quad (3)$$

where the mass term $\mathcal{M}_{\mu\mu'}$ determines the superconducting gap equation, while $\mathcal{T}^{\mu\mu'}_{\delta\gamma}$ controls spatial fluctuations. By introducing the superconducting order parameters $\psi_{1,2}(\mathbf{r},t)$ of $(d_{x^2-y^2}\pm id_{xy})$-waves, we decompose [34, 55]

$$\Phi(\mathbf{r},t)=\psi_1(\mathbf{r},t)\xi_1+\psi_2(\mathbf{r},t)\xi_2, \tag{4}$$

where vectors $\xi_{1,2}=\left(1,e^{\pm i\frac{2\pi}{3}},e^{\pm i\frac{4\pi}{3}}\right)^T/\sqrt{3}$ correspond to the two degenerate $(d_{x^2-y^2}\pm id_{xy})$-wave superconducting phases that span a two-dimensional space and are depicted as a Bloch sphere in Fig. 1, with the $d_{x^2-y^2}\pm id_{xy}$ states being the north and south poles. We will see that an applied vector potential can control their superposition, effectively realizing other points on this Bloch sphere.

We then consider the GL Lagrangian for the subspace of two chiral superconducting order parameters $\psi_{1,2}(\mathbf{r})$, which are the two degenerate ground states of our microscopic model [Eqs. (1) and (2)]. With the decomposition in Eq. (4), the action [Eq. (3)] defines several basis-dependent coefficients via $a_i\equiv\xi_i^\dagger\boldsymbol{\mathcal{M}}\xi_i$ and $c^{ij}_{\delta\gamma}\equiv\xi_i^\dagger\boldsymbol{\mathcal{T}}_{\delta\gamma}\xi_j$. These coefficients are simply parameterized by several real quantities $\{\alpha,\beta,\gamma_1,\lambda_1,\lambda_2\}$ via relations [55]

$$\begin{aligned}&a_1=a_2=\alpha,\quad c^{11}_{\delta\gamma}=c^{22}_{\delta\gamma}=\beta\delta_{\delta\gamma},\\&c^{21}_{xx}=\gamma_1(1-i\sqrt{3}),\quad c^{21}_{yy}=-\gamma_1(1-i\sqrt{3}),\\&c^{21}_{xy}=c^{21}_{yx}=i\gamma_1(1-i\sqrt{3}),\end{aligned} \tag{5}$$

and $c^{ji}_{\delta\gamma}=(c^{ij}_{\delta\gamma})^*$ is guaranteed by Hermiticity. The applied *static* and *uniform* in-plane magnetic field $\mathbf{B}$ induces an effective in-plane vector potential $\mathbf{A}_{x,y}$ via an average over the thickness d of MATBG [47], i.e.,

$$\mathbf{A}_{x,y}\to\sqrt{\langle A^2_{x,y}\rangle}=|B_{y,x}|d/\sqrt{6}, \tag{6}$$

where $\langle\cdots\rangle=\int_0^d dz(\cdots)$ denotes the spatial average over the sample thickness and $\mathbf{A}=\mathbf{z}\times\mathbf{B}$ with the surface normal of the film along the $\hat{\mathbf{z}}$-direction. Including this vector potential via gauge invariance the GL Lagrangian density follows as

$$\begin{aligned}\mathcal{L}_{\text{eff}}(\mathbf{r})=&\,\alpha\sum_{\mu=1,2}|\psi_\mu(\mathbf{r})|^2\\&+\beta\sum_{\nu=x,y}\sum_{\mu=1,2}\left(\partial_\nu+\frac{2e}{i\hbar}\mathbf{A}_\nu\right)\psi^*_\mu\left(\partial_\nu-\frac{2e}{i\hbar}\mathbf{A}_\nu\right)\psi_\mu\\&+\gamma_1(1-i\sqrt{3})\left(\partial_+-\frac{2e}{i\hbar}\mathbf{A}_+\right)\psi^*_2\left(\partial_+-\frac{2e}{i\hbar}\mathbf{A}_+\right)\psi_1\\&+\gamma_1(1+i\sqrt{3})\left(\partial_--\frac{2e}{i\hbar}\mathbf{A}_-\right)\psi_2\left(\partial_-+\frac{2e}{i\hbar}\mathbf{A}_-\right)\psi^*_1\\&+\lambda_1\left(|\psi_1(\mathbf{r})|^2+|\psi_2(\mathbf{r})|^2\right)^2+\lambda_2\left(|\psi_1(\mathbf{r})|^2-|\psi_2(\mathbf{r})|^2\right)^2,\end{aligned} \tag{7}$$

where $\partial_\pm\equiv\partial_x\pm i\partial_y$ and $\mathbf{A}_\pm\equiv\mathbf{A}_x\pm i\mathbf{A}_y$. We stress that the structure of this Lagrangian solely depends on the system's symmetry [1]. Without the magnetic field, the mass term α and spatial fluctuation β are isotropic for either ψ_1 or ψ_2, viz., they are isotropic phases without nematicity. The two chiral states are coupled via the orbital effect of the magnetic field.

Ground state under in-plane magnetic field.—Under the application of an in-plane magnetic field, the ground state can be changed, which is found by minimizing the free energy Eq. (7), yielding

$$\begin{aligned}&\begin{pmatrix}\alpha+\beta\left(2e/\hbar\right)^2\mathbf{A}^2 & -2\gamma_1\left(2e/\hbar\right)^2\mathbf{A}^2e^{-i\varphi}\\ -2\gamma_1\left(2e/\hbar\right)^2\mathbf{A}^2e^{i\varphi} & \alpha+\beta\left(2e/\hbar\right)^2\mathbf{A}^2\end{pmatrix}\begin{pmatrix}\psi_1\\\psi_2\end{pmatrix}\\&+\begin{pmatrix}\Omega_+[\psi_1,\psi_2] & 0\\ 0 & \Omega_-[\psi_1,\psi_2]\end{pmatrix}\begin{pmatrix}\psi_1\\\psi_2\end{pmatrix}=0,\end{aligned} \tag{8}$$

where $\varphi=-\pi/3+2\theta_{\mathbf{A}}$ with $\theta_{\mathbf{A}}=\theta_{\mathbf{B}}+\pi/2$ being the in-plane angle of $\mathbf{A}$ and $\Omega_\pm[\psi_1,\psi_2]\equiv2\lambda_1(|\psi_1|^2+|\psi_2|^2)\pm2\lambda_2(|\psi_1|^2-|\psi_2|^2)$. Without loss of generality, we assume the initial state to be ψ_1 before applying the magnetic field, i.e., a $d+id$ superconductor. After applying the magnetic field, ψ_2 is also mixed into the ground state. However, this admixture is small when the field is weak. On the contrary, when the applied field is sufficiently strong

$$B\gtrsim\frac{\hbar}{2e}\frac{1}{d}\sqrt{\frac{3\alpha}{2(2\gamma_1-\beta}})\equiv B_c, \tag{9}$$

the two order parameters ψ_1 and ψ_2 are driven to be the same in magnitude, and the ground state is no longer a chiral one. We call the complete loss of chirality a phase transition since the symmetry of the phase is completely changed. We note that $B\to0$ when $\alpha\to0$ near T_c. With the ansatz $\psi_2=\psi_1e^{i\varphi}$, we find

$$|\psi_{1,2}|^2=\frac{1}{4\lambda_1}\left[-\alpha+(2\gamma_1-\beta)\left(\frac{2e}{\hbar}\right)^2\mathbf{A}^2\right], \tag{10}$$

which is suppressed by orbital effects when $\beta>2\gamma_1$, as is the case in MATBG (see numerical results below).

The phase in the presence of the magnetic field can be described by a new superconducting order parameter ψ, defined via $\vec{\Phi}=\psi\tilde{\xi}$ with the new basis $\tilde{\xi}=(\xi_1-e^{i\varphi}\xi_2)/\sqrt{2}$, which lies at the equator of the Bloch sphere (Fig. 1). We can describe its Lagrangian via the parameters of Eq. (5). The mass $\tilde{a}=\tilde{\xi}^\dagger\boldsymbol{\mathcal{M}}\tilde{\xi}=\alpha$ is unchanged. The spatial fluctuations are described via coefficients $\tilde{c}_{\delta\gamma}=\tilde{\xi}^\dagger\boldsymbol{\mathcal{T}}_{\delta\gamma}\tilde{\xi}$, leading to

$$\begin{aligned}&\tilde{c}_{xx}=\beta+2\gamma_1\cos(2\theta_{\mathbf{B}}),\\&\tilde{c}_{yy}=\beta-2\gamma_1\cos(2\theta_{\mathbf{B}}),\\&\tilde{c}_{xy}=\tilde{c}_{yx}=2\gamma_1\sin(2\theta_{\mathbf{B}}).\end{aligned} \tag{11}$$

Intriguingly, these coefficients are tunable by the direction of in-plane magnetic field, and are anisotropic along

the $\hat{\mathbf{x}}$- and $\hat{\mathbf{y}}$-directions, viz., correspond to emerging nematicity that breaks the three-fold rotation symmetry in the magnetic-field-driven phase. We can now express the linearized free energy for the order parameter ψ by

$$F = \int d\mathbf{r}\psi^*(\mathbf{r})\mathcal{H}(\hat{\mathbf{r}},t)\psi(\mathbf{r}). \tag{12}$$

where we define

$$\mathcal{H}(\hat{\mathbf{r}},t) = \alpha - \sum_{\mu\nu}\tilde{c}_{\mu\nu}\left(\partial_\mu - \frac{2e}{i\hbar}\mathbf{A}_\mu\right)\left(\partial_\nu - \frac{2e}{i\hbar}\mathbf{A}_\nu\right).$$

We now estimate the magnitude of the in-plane magnetic field to realize the phase transition to the nematic superconducting state in MATBG. With parameters $|V| = t_1 = 4$ meV, $t_2 = 0.2t_1$, $t_3 = 0.05t_1$ and $|\tilde{\mathbf{c}}_\mu| = |\mathbf{c}_\mu| = 14/\sqrt{3}$ nm for the Moiré honeycomb lattice [4, 5], the critical temperature T_c of chiral d-wave superconductivity is calculated by solving $\alpha(T_c) = 0$. T_c is shown in Fig. 2(a) and exhibits a dome with a peak at hole doping $n_h > n_s/2$ where $n_s = 4/\Omega$ characterizes doping four holes in one Moiré unit cell of area Ω [4, 39]. This peak is not at the Van Hove points of

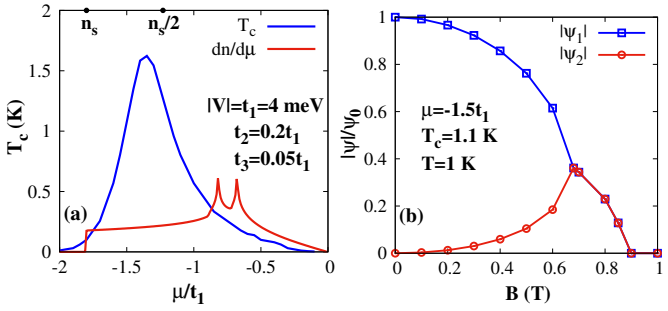

FIG. 2. Calculated critical superconducting temperature and compressibility in (a) and the phase transition induced by in-plane magnetic field when $T \lesssim T_c$ in (b). In (a), the superconducting dome with largest $T_c \approx 1.5$ K recovers the typical features in the experiment [39]. In (b), $\psi_0 = 0.063$ meV and a phase transition at in-plane magnetic field $B \sim 0.6$ T is predicted. The parameters used for the calculation are given in the figure and text.

the band that are characterized by two peaks in compressibility $dn/d\mu$ with our parameters. With a typical hole doping at $\mu = -1.5t_1$, we estimate $T_c \approx 1.1$ K, $\alpha = -10^{-4}/|\mathbf{c}_\mu|^2$ meV$^{-1}\cdot$m^{-2}, $\beta = 2.6$ meV^{-1}, $\gamma_1 = -0.25$ meV^{-1}, and $\lambda_1 = -3\lambda_2 = 0.02/|\mathbf{c}_\mu|^2$ meV$^{-3}\cdot$m^{-2} at temperature $T = 1$ K [52, 55]. With the thickness $d \approx 0.8$ nm of TBG estimated by roughly twice the single-layer one ~ 0.34 nm [56], the two order parameters $\psi_{1,2}$ become close in magnitude when the applied magnetic field $B \gtrsim 0.6$ T, as shown in Fig. 2(b), which is close to the typical value $B_c \approx 0.5$ T found experimentally [39].

Nematic paraconductivity.—The field-driven phase shows a nematic transport response as addressed below. Slightly above the superconducting transition temperature, the conductivity, called paraconductivity, is mainly contributed by the superconductor order parameters since their fluctuation under thermal noise can carry a supercurrent [57, 58]. The measurement of DC resistivity around T_c, as performed in MATBG [39], can thus reflect the fluctuation of the superconducting order parameters and provide information about the pairing symmetry of the superconducting state. To calculate the response to an electric field, the vector potential in $\mathcal{H}(\hat{\mathbf{r}},t)$ is increased by $\mathbf{A}_E = -\mathbf{E}t$, which is the contribution of the applied electric field [58]. Then by the free energy (12), the time-dependent Ginzburg-Landau equation, augmented by thermal noise, is written as [57, 58]

$$\Gamma\partial_t\psi(\mathbf{r},t) = -\mathcal{H}(\hat{\mathbf{r}},t)\psi(\mathbf{r},t) + f(\mathbf{r},t), \tag{13}$$

where Γ is the damping rate for the superconducting order parameter $\psi(\mathbf{r},t)$ and $f(\mathbf{r},t)$ represents thermal noise. We assume that the thermal noise is white with correlation relation $\langle f^*(\mathbf{r},t)f(\mathbf{r}',t')\rangle = 2\Gamma k_BT\delta(\mathbf{r}-\mathbf{r}')\delta(t-t')$ [57, 58]. Via a Fourier transformation, the electric current reads

$$\begin{aligned}\mathbf{J} &\equiv -\frac{\delta F}{\mathcal{S}\delta\mathbf{A}_E}\\ &= -\frac{2k_BT}{\Gamma\mathcal{S}}\sum_{\mathbf{q}}\Lambda(\mathbf{q})\int_{-\infty}^{0}du\exp\left(-\frac{2}{\Gamma}\int_u^0 dt\mathcal{H}(\mathbf{q},t)\right),\end{aligned} \tag{14}$$

where $\mathcal{S}$ is the sample area and $\Lambda(\mathbf{q}) \equiv \partial\mathcal{H}(\mathbf{q},t)/\partial\mathbf{A}_E|_{\mathbf{A}_E\to 0}$. From this the paraconductivity is determined in linear response to be

$$\sigma_{ij} = k_BT\frac{e^2\Gamma}{2\pi\hbar^2\alpha}\frac{\tilde{c}_{ij}}{\sqrt{\beta^2-4\gamma_1^2}}, \tag{15}$$

which is a tensor that exhibits an anomalous Hall response. This emerging anomalous Hall effect is unique to the magnetic-field-driven phase since it is absent in the chiral superconducting phase without magnetic field, which follows an isotropic paraconductivity $\sigma^c_{ij} = k_BTe^2\Gamma/(2\pi\hbar^2\alpha)\delta_{ij}$. In particular, when the electric field is applied along the $\hat{\mathbf{x}}$-direction in the coordinate system defined in Fig. 3(a), the induced current along the $\hat{\mathbf{x}}$-direction is modulated as $\tilde{c}_{xx}$, and there is a Hall response with the current along the $\hat{\mathbf{y}}$-direction being modulated as $\tilde{c}_{yx}$. They are both nematic with a two-fold anisotropy [Eq. (11)].

We estimate the paraconductivity by choosing $\Gamma = \eta\alpha\hbar/(k_BT_c)$ with a factor η of order 1 [59, 60], leading to a universal paraconductivity $\sigma_{ij} = \eta\sigma_q\tilde{c}_{ij}/\sqrt{\beta^2-4\gamma_1^2}$ with $\sigma_q = e^2/(2\pi\hbar) = 3.87\times10^{-5}$ S being the conductance quantum. With the parameters at $\mu = -1.5t_1$ and $T = 1.2$ K, we plot σ_{ij}/σ_q in Fig. 3(b) with $B \gtrsim 0.6$ T

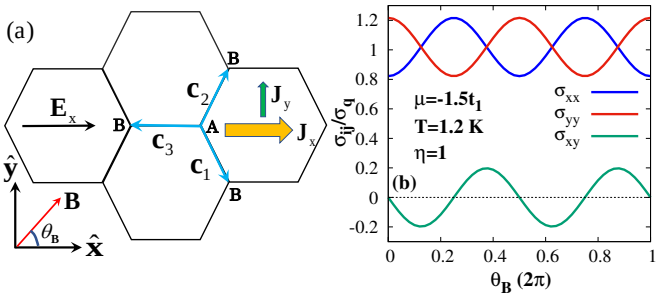

FIG. 3. Nematic conductivities and Hall response of the driven phase when the in-plane magnetic field is larger than a critical one. We address the coordinate and Hall response in (a) and plot the dependence of the conductivities on the magnetic-field direction in (b). The parameters used for calculation are given in the figure and text.

and η taken to be 1. The conductivities oscillate with respect to the magnetic field with period of π, thus exhibiting a two-fold anisotropy. The amplitude of the oscillation is determined by $|\gamma_1|$ that may depend on the behind microscopic mechanism. The direction of the in-plane magnetic field tunes the sign of σ_{xy} and hence the direction of the Hall current, which also could provide an intriguing functionality for future applications.

Discussion.—We have demonstrated nematicity in the paraconductivity that emerges in two-dimensional chiral superconductors under an in-plane magnetic field. This effect is particularly instructive for the chiral d-wave superconducting state of the honeycomb lattice in that the driven phase shows two-fold anisotropy that breaks the three-fold one of the lattice. Furthermore, the magnetic-field–driven nematic phase shows an anomalous Hall effect in a non-ferromagnetic system. The underlying mechanism relies on the hybridization of chiral order parameters by an in-plane vector potential with shifted nodes of the gap in the driven phase, which could be directly tracked by STM [61]. Our work has direct implications for the pairing symmetry of superconductivity in MATBG, but can also be extended to other multicomponent superconductors.

TY and MAS acknowledge financial support by Deutsche Forschungsgemeinschaft through the Emmy Noether program (SE 2558/2). DMK acknowledges support by the Deutsche Forschungsgemeinschaft (DFG, German Research Foundation) via RTG 1995, within the Priority Program SPP 2244 “2DMP” and Germany’s Excellence Strategy - Cluster of Excellence Matter and Light for Quantum Computing (ML4Q) EXC 2004/1 - 390534769. AR acknowledges support from the European Research Council (ERC- 2015-AdG-694097), UPV/EHU Grupos Consolidados (IT1249-19) and the Cluster of Excellence ‘CUI: Advanced Imaging of Matter’ of the Deutsche Forschungsgemeinschaft (DFG) - EXC 2056 - project ID 390715994. The Flatiron Institute is a division of the Simons Foundation. We acknowledge support from the Max Planck-New York City Center for Non-Equilibrium Quantum Phenomena.

[1] M. Sigrist and K. Ueda, Rev. Mod. Phys. **63**, 239 (1991).
[2] C. C. Tsuei and J. R. Kirtley, Rev. Mod. Phys. **72**, 969 (2000).
[3] A. P. Mackenzie and Y. Maeno, Rev. Mod. Phys. **75**, 657 (2003).
[4] Y. Cao, V. Fatemi, S. Fang, K. Watanabe, T. Taniguchi, E. Kaxiras, and P. Jarillo-Herrero, Nature (London) **556**, 43 (2018).
[5] Y. Cao, V. Fatemi, A. Demir, S. Fang, S. L. Tomarken, J. Y. Luo, J. D. Sanchez-Yamagishi, K. Watanabe, T. Taniguchi, E. Kaxiras *et al.*, Nature (London) **556**, 80 (2018).
[6] M. Yankowitz, S. Chen, H. Polshyn, Y. Zhang, K. Watanabe, T. Taniguchi, D. Graf, A. F. Young, and C. R. Dean, Science **363**, 1059 (2019).
[7] X. Lu, P. Stepanov, W. Yang, M. Xie, M. A. Aamir, I. Das, C. Urgell, K. Watanabe, T. Taniguchi, G. Zhang *et al.*, Nature (London) **574**, 653 (2019).
[8] F. Wu, A. H. MacDonald, and I. Martin, Phys. Rev. Lett. **121**, 257001 (2018).
[9] Y. W. Choi and H. J. Choi, Phys. Rev. B **98**, 241412(R) (2018).
[10] T. J. Peltonen, R. Ojajärvi, and T. T. Heikkilä, Phys. Rev. B **98**, 220504(R) (2018).
[11] M. Angeli, E. Tosatti, and M. Fabrizio, Phys. Rev. X **9**, 041010 (2019).
[12] B. Lian, Z. Wang, and B. A. Bernevig, Phys. Rev. Lett. **122**, 257002 (2019).
[13] R. Samajdar and M. S. Scheurer, Phys. Rev. B **102**, 064501 (2020).
[14] J. W. F. Venderbos and R. M. Fernandes, Phys. Rev. B **98**, 245103 (2018).
[15] H. Isobe, N. F. Q. Yuan, and L. Fu, Phys. Rev. X **8**, 041041 (2018).
[16] Y. Sherkunov and J. J. Betouras, Phys. Rev. B **98**, 205151 (2018).
[17] Y.-P. Lin and R. M. Nandkishore, Phys. Rev. B **98**, 214521 (2018).
[18] J. F. Dodaro, S. A. Kivelson, Y. Schattner, X. Q. Sun, and C. Wang, Phys. Rev. B **98**, 075154 (2018).
[19] C. Xu and L. Balents, Phys. Rev. Lett. **121**, 087001 (2018).
[20] M. Fidrysiak, M. Zegrodnik, and J. Spałek, Phys. Rev. B **98**, 085436 (2018).
[21] C.-C. Liu, L.-D. Zhang, W.-Q. Chen, and F. Yang, Phys. Rev. Lett. **121**, 217001 (2018).
[22] Y. Su and S.-Z. Lin, Phys. Rev. B **98**, 195101 (2018).
[23] D. M. Kennes, J. Lischner, and C. Karrasch, Phys. Rev. B **98**, 241407(R) (2018).
[24] H. C. Po, L. Zou, A. Vishwanath, and T. Senthil, Phys. Rev. X **8**, 031089 (2018).
[25] Y.-Z. You and A. Vishwanath, npj Quantum Materials **4**, 1 (2019).
[26] L. Classen, C. Honerkamp, and M. M. Scherer, Phys.

Rev. B **99**, 195120 (2019).
[27] S. Ray, J. Jung, and T. Das, Phys. Rev. B **99**, 134515 (2019).
[28] J. González and T. Stauber, Phys. Rev. Lett. **122**, 026801 (2019).
[29] Y.-P. Lin and R. M. Nandkishore, Phys. Rev. B **100**, 085136 (2019).
[30] M. Claassen, D. M. Kennes, M. Zingl, M. A. Sentef, and A. Rubio, Nat. Phys. **15**, 766 (2019).
[31] W. Chen, Y. Chu, T. Huang, and T. Ma, Phys. Rev. B **101**, 155413 (2020).
[32] A. Fischer, L. Klebl, C. Honerkamp, and D. M. Kennes, arXiv:2008.12532.
[33] R. Nandkishore, L. S. Levitov, and A. V. Chubukov, Nat. Phys. **8**, 158 (2012).
[34] A. M. Black-Schaffer and C. Honerkamp, J. Phys. Condens. Matter **26**, 423201 (2014).
[35] G. M. Luke, A. Keren, L. P. Le, W. D. Wu, Y. J. Uemura, D. A. Bonn, L. Taillefer, and J. D. Garrett, Phys. Rev. Lett. **71**, 1466 (1993).
[36] R. Joynt and L. Taillefer, Rev. Mod. Phys. **74**, 235 (2002).
[37] K. E. Avers, W. J. Gannon, S. J. Kuhn, W. P. Halperin, J. A. Sauls, L. DeBeer-Schmitt, C. D. Dewhurst, J. Gavilano, G. Nagy, U. Gasser, and M. R. Eskildsen, Nat. Phys. **16**, 531 (2020).
[38] L. Jiao, S. Howard, S. Ran, Z. Y. Wang, J. O. Rodriguez, M. Sigrist, Z. Q. Wang, N. P. Butch, and V. Madhavan, Nature **579**, 523 (2020).
[39] Y. Cao, D. R.-Legrain, J. M. Park, F. N. Yuan, K. Watanabe, T. Taniguchi, R. M. Fernandes, L. Fu, and P. J.-Herrero, arXiv:2004.04148.
[40] D. V. Chichinadze, L. Classen, and A. V. Chubukov, Phys. Rev. B **101**, 224513 (2020).
[41] Y. X. Wang, J. Kang, and R. M. Fernandes, arXiv:2009.01237.
[42] A. Kerelsky, L. J. McGilly, D. M. Kennes, L. D. Xian, M. Yankowitz, S. W. Chen, K. Watanabe, T. Taniguchi, J. Hone, C. Dean, A. Rubio, and A. N. Pasupathy, Nature (London) **572**, 95 (2019).
[43] Y. Choi, J. Kemmer, Y. Peng, A. Thomson, H. Arora, R. Polski, Y. Zhang, H. Ren, J. Alicea, G. Refael, F. von Oppen, K. Watanabe, T. Taniguchi, and S. Nadj-Perge, Nat. Phys. **15**, 1174 (2019).
[44] Y. Jiang, X. Lai, K. Watanabe, T. Taniguchi, K. Haule, J. Mao, and E. Y. Andrei, Nature (London) **573**, 91 (2019).
[45] C. R.-Verdú, S. Turkel, L. Song, L. Klebl, R. Samajdar, M. S. Scheurer, J. W. F. Venderbos, K. Watanabe, T. Taniguchi, H. Ochoa, L. Xian, D. Kennes, R. M. Fernandes, Á. Rubio, and A. N. Pasupathy, arXiv:2009.11645.
[46] P. Stepanov, I. Das, X. Lu, A. Fahimniya, K. Watanabe, T. Taniguchi, F. H. L. Koppens, J. Lischner, L. Levitov, and D. K. Efetov, Nature **583**, 375 (2020).
[47] V. Vadimov and M. Silaev, Phys. Rev. Lett. **111**, 177001 (2013).
[48] A. Pustogow, Y. Luo, A. Chronister, Y. S. Su, D. A. Sokolov, F. Jerzembeck, A. P. Mackenzie, C. W. Hicks, N. Kikugawa, S. Raghu, E. D. Bauer, and S. E. Brown, Nature (London) **574**, 72 (2019).
[49] S. Ghosh *et al.*, Nat. Phys. (2020), https://www.nature.com/articles/s41567-020-1032-4.
[50] S. Benhabib *et al.*, Nat. Phys. (2020), https://www.nature.com/articles/s41567-020-1033-3.
[51] N. Nagaosa, J. Sinova, S. Onoda, A. H. MacDonald, and N. P. Ong, Rev. Mod. Phys. **82**, 1539 (2010).
[52] N. F. Q. Yuan and L. Fu, Phys. Rev. B **98**, 045103 (2018).
[53] T. Yu, M. Claassen, D. M. Kennes, and M. A. Sentef, arXiv:2010.00838.
[54] A. Altland and B. Simons, *Condensed Matter Field Theory* (Cambridge University Press, Cambridge, England, 2010).
[55] See Supplemental Material at [...] for detailed derivation of effective GL Lagrangian for the superconducting order parameters and estimation of GL parameters by microscopic model.
[56] A. H. Castro Neto, F. Guinea, N. M. R. Peres, K. S. Novoselov, and A. K. Geim, Rev. Mod. Phys. **81**, 109 (2009).
[57] W. J. Skocpol and M. Tinkham, Rep. Prog. Phys. **38**, 1049 (1975).
[58] R. Wakatsuki, Y. Saito, S. Hoshino, Y. M. Itahashi, T. Ideue, M. Ezawa, Y. Iwasa, and N. Nagaosa, Sci. Adv. **3**, e1602390 (2017).
[59] L. P. Gor'kov, Sov. Phys. JETP **9**, 1364 (1959).
[60] N. Kopnin, *Theory of Nonequilibrium Superconductivity* (Oxford University Press, New York, 2001).
[61] Ø. Fischer, M. Kugler, I. Maggio-Aprile, C. Berthod, and C. Renner, Rev. Mod. Phys. **79**, 353 (2007).

Nematicity Arising from a Chiral Superconducting Ground State in Magic-Angle Twisted Bilayer Graphene under In-Plane Magnetic Fields: Supplemental Material

Tao Yu,[1] Dante M. Kennes,[2,1] Angel Rubio,[1,3,4] and Michael A. Sentef[1]

[1] *Max Planck Institute for the Structure and Dynamics of Matter, Luruper Chaussee 149, 22761 Hamburg, Germany*

[2] *Institut für Theorie der Statistischen Physik, RWTH Aachen, 52056 Aachen, Germany*

[3] *Center for Computational Quantum Physics (CCQ), The Flatiron Institute, 162 Fifth Avenue, New York, New York 10010, USA*

[4] *Nano-Bio Spectroscopy Group, Departamento de Física de Materiales, Universidad del País Vasco, 20018 San Sebastian, Spain*

(Dated: January 6, 2021)

I. EFFECTIVE LAGRANGIAN

We employ the Yuan-Fu model [1] to describe the flat band in MATBG. Figure S1 gives a brief description of the model and defines the symbols. The moiré honeycomb lattice has two sites in a unit cell, i.e., A site and B site, labeled, respectively, by "i" and "j" below. At every site, there are two p-orbitals $\{p_x, p_y\}$. The two primitive vectors of the lattice are $\mathbf{a}_1 = \mathbf{c}_1 - \mathbf{c}_3$ and $\mathbf{a}_2 = \mathbf{c}_2 - \mathbf{c}_3$ in terms of three nearest bonding vectors $\mathbf{c}_{1,2,3}$; $\mathbf{d}_{\mu=\{1,2,3\}}$ are three fifth neighboring bonding vectors that connect two A sites or two B sites. Yuan-Fu model, with a suppression of spin index, gives

$$\begin{aligned}\hat{H}_{\mathrm{TB}} = &-\mu\sum_i \hat{\mathbf{a}}_i^\dagger\cdot\hat{\mathbf{a}}_i - \mu\sum_j \hat{\mathbf{b}}_j^\dagger\cdot\hat{\mathbf{b}}_j \\ &+ t_1\sum_{\langle ij\rangle}(\hat{\mathbf{a}}_i^\dagger\cdot\hat{\mathbf{b}}_j + \mathrm{H.c.}) + t_2\sum_{\langle ii'\rangle_5}(\hat{\mathbf{a}}_i^\dagger\cdot\hat{\mathbf{a}}_{i'} + \mathrm{H.c.}) + t_2\sum_{\langle jj'\rangle_5}(\hat{\mathbf{b}}_j^\dagger\cdot\hat{\mathbf{b}}_{j'} + \mathrm{H.c.}) \\ &+ t_3\sum_{\langle ii'\rangle_5}\left[(\hat{\mathbf{a}}_i^\dagger\times\hat{\mathbf{a}}_{i'})_z + \mathrm{H.c.}\right] + t_3\sum_{\langle jj'\rangle_5}\left[(\hat{\mathbf{b}}_j^\dagger\times\hat{\mathbf{b}}_{j'})_z + \mathrm{H.c.}\right],\end{aligned} \tag{S1}$$

where $\hat{\mathbf{a}}_i = (\hat{a}_{ix}, \hat{a}_{iy})$ and $\hat{\mathbf{b}}_j = (\hat{b}_{jx}, \hat{b}_{jy})$ are the operators of different sites and orbitals, μ is the chemical potential and $t_{i=1,2,3}$ are the hopping parameters. Particularly, only t_3-term mixes the x- and y-orbitals.

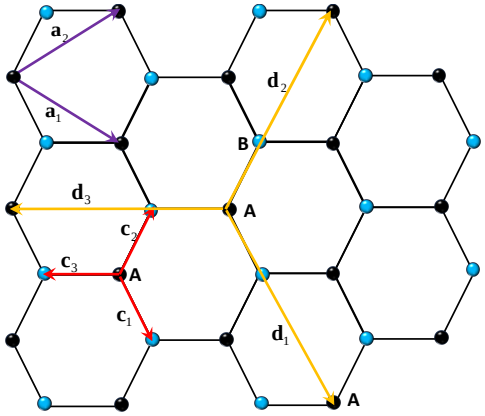

FIG. S1. Honeycomb moiré lattice. Parameters are defined in the text.

This model can be solved analytically. In the momentum space with $\hat{\mathbf{a}}_i = \frac{1}{\sqrt{N}}\sum_{\mathbf{k}} e^{i\mathbf{k}\cdot\mathbf{R}_i}\hat{\mathbf{a}}_{\mathbf{k}}$ and $\hat{\mathbf{b}}_j = \frac{1}{\sqrt{N}}\sum_{\mathbf{k}} e^{i\mathbf{k}\cdot\mathbf{R}_j}\hat{\mathbf{b}}_{\mathbf{k}}$, the Hamiltonian

$$\begin{aligned}\hat{H}_{\mathrm{TB}} = &-\mu\sum_{\mathbf{k}}\hat{\mathbf{a}}_{\mathbf{k}}^\dagger\cdot\hat{\mathbf{a}}_{\mathbf{k}} - \mu\sum_{\mathbf{k}}\hat{\mathbf{b}}_{\mathbf{k}}^\dagger\cdot\hat{\mathbf{b}}_{\mathbf{k}} \\ &+ t_1\sum_{\mathbf{k}} f(\mathbf{k})\hat{\mathbf{a}}_{\mathbf{k}}^\dagger\cdot\hat{\mathbf{b}}_{\mathbf{k}} + t_2\sum_{\mathbf{k}} g(\mathbf{k})(\hat{\mathbf{a}}_{\mathbf{k}}^\dagger\cdot\hat{\mathbf{a}}_{\mathbf{k}} + \hat{\mathbf{b}}_{\mathbf{k}}^\dagger\cdot\hat{\mathbf{b}}_{\mathbf{k}}) + t_3\sum_{\mathbf{k}} g(\mathbf{k})\left[(\hat{\mathbf{a}}_{\mathbf{k}}^\dagger\times\hat{\mathbf{a}}_{\mathbf{k}})_z + (\hat{\mathbf{b}}_{\mathbf{k}}^\dagger\times\hat{\mathbf{b}}_{\mathbf{k}})_z\right] + \mathrm{H.c.},\end{aligned} \tag{S2}$$

where $f(\mathbf{k}) = \sum_{\delta=1,2,3} e^{i\mathbf{k}\cdot\mathbf{c}_\delta}$ and $g(\mathbf{k}) = \sum_{\delta=1,2,3} e^{i\mathbf{k}\cdot\mathbf{d}_\delta}$, which, under the basis $\hat{\Psi}_{\mathbf{k}} = (\hat{a}_{\mathbf{k}x}, \hat{a}_{\mathbf{k}y}, \hat{b}_{\mathbf{k}x}, \hat{b}_{\mathbf{k}y})^T$, reads $\mathcal{H}(\mathbf{k}) = -\mu + t_2(g_{\mathbf{k}} + g_{-\mathbf{k}}) + \begin{pmatrix} 0 & t_3(g_{\mathbf{k}} - g_{-\mathbf{k}}) & t_1 f_{\mathbf{k}} & 0 \\ t_3(g_{-\mathbf{k}} - g_{\mathbf{k}}) & 0 & 0 & t_1 f_{\mathbf{k}} \\ t_1 f_{-\mathbf{k}} & 0 & 0 & t_3(g_{\mathbf{k}} - g_{-\mathbf{k}}) \\ 0 & t_1 f_{-\mathbf{k}} & t_3(g_{-\mathbf{k}} - g_{\mathbf{k}}) & 0 \end{pmatrix}$. This matrix is

brought to be block diagonal under the chiral basis

$$\begin{pmatrix}\hat{a}_{\mathbf{k}x}\\ \hat{a}_{\mathbf{k}y}\\ \hat{b}_{\mathbf{k}x}\\ \hat{b}_{\mathbf{k}y}\end{pmatrix}=\frac{1}{\sqrt{2}}\begin{pmatrix}1 & 1 & 0 & 0\\ -i & i & 0 & 0\\ 0 & 0 & 1 & 1\\ 0 & 0 & -i & i\end{pmatrix}\begin{pmatrix}\hat{a}_{\mathbf{k}+}\\ \hat{a}_{\mathbf{k}-}\\ \hat{b}_{\mathbf{k}+}\\ \hat{b}_{\mathbf{k}-}\end{pmatrix}, \tag{S3}$$

where " $\pm$ " holds angular momentum ± 1, respectively. With basis $(\hat{a}_{\mathbf{k}\pm}, \hat{b}_{\mathbf{k}\pm})^T$, the subspace is explicitly written by

$$h_{\pm}(\mathbf{k}) = -\mu + t_2(g_{\mathbf{k}} + g_{-\mathbf{k}}) \pm it_3(g_{-\mathbf{k}} - g_{\mathbf{k}}) + \begin{pmatrix} 0 & t_1 f_{\mathbf{k}} \\ t_1 f_{-\mathbf{k}} & 0, \end{pmatrix}. \tag{S4}$$

For the pairing interaction, we look into the Hamiltonian of the form [2–4]

$$\hat{H}_{\text{int}} \simeq \sum_{\alpha=\pm}\sum_{\mathbf{k}\mathbf{k}'} V_\alpha(\mathbf{k}-\mathbf{k}')\left[\hat{a}^\dagger_{\alpha\uparrow}(\mathbf{k})\hat{b}^\dagger_{\alpha\downarrow}(-\mathbf{k}) - \hat{a}^\dagger_{\alpha\downarrow}(\mathbf{k})\hat{b}^\dagger_{\alpha\uparrow}(-\mathbf{k})\right]\left[\hat{b}_{\alpha\downarrow}(-\mathbf{k}')\hat{a}_{\alpha\uparrow}(\mathbf{k}') - \hat{b}_{\alpha\uparrow}(-\mathbf{k}')\hat{a}_{\alpha\downarrow}(\mathbf{k}')\right], \tag{S5}$$

where we express the pairing potential

$$V_\alpha(\mathbf{k}-\mathbf{k}') = \frac{V_\alpha}{N}\sum_{\mu=\{1,2,3\}} e^{i(\mathbf{k}-\mathbf{k}')\cdot\tilde{\mathbf{c}}_\mu}. \tag{S6}$$

To construct the Lagrangian of the superconducting order parameter, we use a continuous description that is equivalent to the above lattice model via the continuous field operators $\hat{a}_\alpha(\mathbf{r}) = \frac{1}{\sqrt{S}}\sum_{\mathbf{k}}\hat{a}_\alpha(\mathbf{k})e^{i\mathbf{k}\cdot\mathbf{r}}$ and $\hat{b}_\alpha(\mathbf{r}) = \frac{1}{\sqrt{S}}\sum_{\mathbf{k}}\hat{b}_\alpha(\mathbf{k})e^{i\mathbf{k}\cdot\mathbf{r}}$, where $S = N\Omega$ is the area of the honeycomb lattices with $\Omega = \sqrt{3}a^2/2 = 3\sqrt{3}c^2/2$ being the area of one unit cell in which $a = |\mathbf{a}_1| = |\mathbf{a}_2|$ and $c = |\mathbf{c}_\delta|$. Then interaction Eq. (S5) corresponds to

$$\hat{H}_{\text{int}} \simeq \Omega\sum_\mu\sum_\alpha V_\alpha\int d\mathbf{r}\left[\hat{b}^\dagger_{\alpha\uparrow}(\mathbf{r}_\mu)\hat{a}^\dagger_{\alpha\downarrow}(\mathbf{r}) - \hat{b}^\dagger_{\alpha\downarrow}(\mathbf{r}_\mu)\hat{a}^\dagger_{\alpha\uparrow}(\mathbf{r})\right]\left[\hat{a}_{\alpha\downarrow}(\mathbf{r})\hat{b}_{\alpha\uparrow}(\mathbf{r}_\mu) - \hat{a}_{\alpha\uparrow}(\mathbf{r})\hat{b}_{\alpha\downarrow}(\mathbf{r}_\mu)\right], \tag{S7}$$

where $\mathbf{r}_\mu \equiv \mathbf{r} + \tilde{\mathbf{c}}_\mu$. The subspace now is independent that allows us to omit the index "α" for simplicity below. With the field operator $\hat{\Psi}(\mathbf{r}) = (\hat{a}_\uparrow(\mathbf{r}), \hat{b}_\uparrow(\mathbf{r}), \hat{a}^\dagger_\downarrow(\mathbf{r}), \hat{b}^\dagger_\downarrow(\mathbf{r}))^T$, the free part of the Hamiltonian becomes

$$\hat{H}_0 = \int d\mathbf{r}\hat{\Psi}^\dagger(\mathbf{r})\begin{pmatrix}h(\hat{\mathbf{k}}) & O\\ O & -h^\dagger(-\hat{\mathbf{k}})\end{pmatrix}\hat{\Psi}(\mathbf{r}). \tag{S8}$$

Now we define two 4×4 matrix $\tau_1 = \mathcal{P}_{23}$ and $\tau_2 = \mathcal{P}_{14}$ via relations $\hat{\Psi}^\dagger(\mathbf{r}_\mu)\tau_1\hat{\Psi}(\mathbf{r}) = \hat{b}^\dagger_\uparrow(\mathbf{r}_\mu)\hat{a}^\dagger_\downarrow(\mathbf{r})$ and $\hat{\Psi}^\dagger(\mathbf{r})\tau_2\hat{\Psi}(\mathbf{r}_\mu) = -\hat{b}^\dagger_\downarrow(\mathbf{r}_\mu)\hat{a}^\dagger_\uparrow(\mathbf{r}) = \hat{a}^\dagger_\uparrow(\mathbf{r})\hat{b}^\dagger_\downarrow(\mathbf{r}_\mu)$, where $\mathcal{P}_{ij}$ represents a matrix with only one non-zero element $(i,j) = 1$, with which the interaction Hamiltonian becomes

$$\hat{H}_{\text{int}} = \Omega\sum_\mu V\int d\mathbf{r}\left[\hat{\Psi}^\dagger(\mathbf{r}_\mu)\tau_1\hat{\Psi}(\mathbf{r}) + \hat{\Psi}^\dagger(\mathbf{r})\tau_2\hat{\Psi}(\mathbf{r}_\mu)\right]\left[\hat{\Psi}^\dagger(\mathbf{r})\tau_1^T\hat{\Psi}(\mathbf{r}_\mu) + \hat{\Psi}^\dagger(\mathbf{r}_\mu)\tau_2^T\hat{\Psi}(\mathbf{r})\right]. \tag{S9}$$

With the Grassman field $\overline{\Psi}(\mathbf{r},t) = \big(\overline{a}_\uparrow(\mathbf{r}), \overline{b}_\uparrow(\mathbf{r}), a_\downarrow(\mathbf{r}), b_\downarrow(\mathbf{r})\big)$, the action is expressed as

$$\begin{aligned}S = &\int_0^\beta d\tau d\mathbf{r}\overline{\Psi}(\mathbf{r},\tau)\partial_\tau\Psi(\mathbf{r},\tau) + \int_0^\beta d\tau d\mathbf{r}\overline{\Psi}(\mathbf{r},\tau)H_0(\hat{\mathbf{k}})\Psi(\mathbf{r},\tau)\\ &- \Omega\sum_\mu V\int_0^\beta d\tau\int d\mathbf{r}\left[\overline{\Psi}(\mathbf{r}_\mu)\tau_1\Psi(\mathbf{r}) + \overline{\Psi}(\mathbf{r})\tau_2\Psi(\mathbf{r}_\mu)\right]\left[\overline{\Psi}(\mathbf{r})\tau_1^T\Psi(\mathbf{r}_\mu) + \overline{\Psi}(\mathbf{r}_\mu)\tau_2^T\Psi(\mathbf{r})\right].\end{aligned} \tag{S10}$$

We introduce the complex Bose field $\phi(\mathbf{r},\mathbf{r}_\mu)$ by Hubbard-Stratonovich transformation

$$1=\int \mathcal{D}\phi(\mathbf{r},\mathbf{r}_\mu)\mathcal{D}\overline{\phi}(\mathbf{r},\mathbf{r}_\mu)\exp\left(-\int_0^\beta d\tau\sum_\mu\int d\mathbf{r}\overline{\phi}(\mathbf{r},\mathbf{r}_\mu)\frac{1}{V\Omega}\phi(\mathbf{r},\mathbf{r}_\mu)\right),$$

with which the action

$$\begin{aligned}S=&\int_0^\beta d\tau d\mathbf{r}\overline{\Psi}(\mathbf{r},\tau)\left(\partial_\tau+H_0(\hat{\mathbf{k}})\right)\Psi(\mathbf{r},\tau)+\sum_\mu\int_0^\beta d\tau d\mathbf{r}\overline{\phi}(\mathbf{r},\mathbf{r}_\mu)\frac{1}{V\Omega}\phi(\mathbf{r},\mathbf{r}_\mu)\\&+\sum_\mu\int_0^\beta d\tau d\mathbf{r}\overline{\phi}(\mathbf{r},\mathbf{r}_\mu)\left(\overline{\Psi}(\mathbf{r})\tau_1^T\Psi(\mathbf{r}_\mu)+\overline{\Psi}(\mathbf{r}_\mu)\tau_2^T\Psi(\mathbf{r})\right)+\sum_\mu\int_0^\beta d\tau d\mathbf{r}\left(\overline{\Psi}(\mathbf{r}_\mu)\tau_1\Psi(\mathbf{r})+\overline{\Psi}(\mathbf{r})\tau_2\Psi(\mathbf{r}_\mu)\right)\phi(\mathbf{r},\mathbf{r}_\mu).\end{aligned}$$

We integrate out the fermion degree of freedom in momentum-frequency space with the fermion field $\Psi(\tau,\mathbf{r})=\frac{1}{\sqrt{\beta}}\frac{1}{\sqrt{S}}\sum_{\mathbf{k}}\sum_{\omega_n}\Psi(\omega_n,\mathbf{k})e^{-i\omega_n\tau}e^{i\mathbf{k}\cdot\mathbf{r}}$ and the boson field, with respect to the *center-of-mass* coordinate $\mathbf{r}+\mathbf{r}_\mu/2$, $\phi(\tau,\mathbf{r},\mathbf{r}+\tilde{\mathbf{c}}_\mu)=\frac{1}{\sqrt{\beta}}\frac{1}{\sqrt{S}}\sum_{\mathbf{k}}\sum_{\omega_m}\phi(\omega_m,\mathbf{k})e^{-i\omega_n\tau}e^{i\mathbf{k}\cdot(\mathbf{r}+\tilde{\mathbf{c}}_\mu/2)}$. With $k=\{\omega_n,\mathbf{k}\}$ and $q=\{\omega_m,\mathbf{q}\}$, the action

$$\begin{aligned}S=&\sum_\mu\sum_q\overline{\phi}_\mu(q)\frac{1}{\tilde{V}}\phi_\mu(q)\\&+\sum_{kk'}\overline{\Psi}_k\Big\{\big[-i\omega_n+H_0(\mathbf{k})\big]\delta_{kk'}+\frac{1}{\sqrt{S\beta}}\sum_\mu\big[\overline{\phi}_\mu(k'-k)(e^{i\boldsymbol{\kappa}\cdot\tilde{\mathbf{c}}_\mu}\tau_1^T+e^{-i\boldsymbol{\kappa}\cdot\tilde{\mathbf{c}}_\mu}\tau_2^T)\\&+\phi_\mu(k-k')(e^{-i\boldsymbol{\kappa}\cdot\tilde{\mathbf{c}}_\mu}\tau_1+e^{i\boldsymbol{\kappa}\cdot\tilde{\mathbf{c}}_\mu}\tau_2)\big]\Big\}\Psi_{k'},\end{aligned}\tag{S11}$$

where $\tilde{V}\equiv V/N$ and $\boldsymbol{\kappa}\equiv(\mathbf{k}+\mathbf{k}')/2$ denotes the center-of-mass momentum. For convenience, we define the operator $\hat{Q}$ via matrix elements

$$\langle k|\hat{Q}|k'\rangle=\frac{1}{\sqrt{S\beta}}\sum_\mu\left[\overline{\phi}_\mu(k'-k)\left(e^{i\boldsymbol{\kappa}\cdot\tilde{\mathbf{c}}_\mu}\tau_1^T+e^{-i\boldsymbol{\kappa}\cdot\tilde{\mathbf{c}}_\mu}\tau_2^T\right)+\phi_\mu(k-k')\left(e^{-i\boldsymbol{\kappa}\cdot\tilde{\mathbf{c}}_\mu}\tau_1+e^{i\boldsymbol{\kappa}\cdot\tilde{\mathbf{c}}_\mu}\tau_2\right)\right],$$

and the operator $\hat{G}_0^{-1}[\phi]=i\hat{\omega}-\hat{H}_0$ with elements $\langle k|(i\hat{\omega}-\hat{H}_0)|k'\rangle=(i\omega_n-\hat{H}_0(\mathbf{k}))\delta_{kk'}$. By integrating out the Fermion field, we arrive at the partition function

$$Z=\int\mathcal{D}\overline{\phi}_\mu(q)\mathcal{D}\phi_\mu(q)\exp\left(-\sum_\mu\sum_q\overline{\phi}_\mu(q)\frac{1}{\tilde{V}}\phi_\mu(q)+\mathrm{tr}\ln\left((-i\hat{\omega}+\hat{H}_0)+\hat{Q}\right)\right),$$

with $\mathrm{tr}(...)=\sum_k\langle k|...|k\rangle$. The effective action becomes

$$S_{\text{eff}}[\overline{\phi},\phi]=\sum_\mu\sum_q\overline{\phi}_\mu(q)\frac{1}{\tilde{V}}\phi_\mu(q)-\mathrm{Tr}\ln\Big(-\hat{G}_0^{-1}(1-\hat{G}_0\hat{Q})\Big).\tag{S12}$$

When the order parameter is small, we expand

$$-\mathrm{Tr}\ln\left(-\hat{G}_0^{-1}(1-\hat{G}_0\hat{Q})\right)\to\frac{1}{2}\mathrm{Tr}(\hat{G}_0\hat{Q}\hat{G}_0\hat{Q})=\frac{1}{2}\sum_{kk'}\mathrm{tr}\left(G_k^0Q_{k,k'}G_{k'}^0Q_{k',k}\right),$$

and arrive at the effective action

$$S_{\text{eff}}[\overline{\phi},\phi]=\sum_{\mu q}\overline{\phi}_\mu(q)\frac{1}{\tilde{V}}\phi_\mu(q)+\frac{1}{\beta}\frac{1}{S}\sum_{kq}\sum_{\mu\mu'}B_{\mu\mu'}\left(k-\frac{q}{2},k+\frac{q}{2}\right)\overline{\phi}_\mu(q)\phi_{\mu'}(q)+O(\phi^4),\tag{S13}$$

where

$$B_{\mu\mu'}\left(k-\frac{q}{2},k+\frac{q}{2}\right)=\mathrm{tr}\left(G^0_{k-\frac{q}{2}}(e^{i\mathbf{k}\cdot\tilde{\mathbf{c}}_\mu}\tau_1^T+e^{-i\mathbf{k}\cdot\tilde{\mathbf{c}}_\mu}\tau_2^T)G^0_{k+\frac{q}{2}}(e^{-i\mathbf{k}\cdot\tilde{\mathbf{c}}_{\mu'}}\tau_1+e^{i\mathbf{k}\cdot\tilde{\mathbf{c}}_{\mu'}}\tau_2)\right).\tag{S14}$$

Assuming a small $\mathbf{q}$, we define

$$\begin{aligned}
&\frac{1}{S}\frac{1}{\beta}\sum_{k} B^{\mu\mu'}_{k,k} + \frac{1}{V\Omega}\delta_{\mu\mu'} \equiv \mathcal{M}^{\mu\mu'}(q=0),\\
&\frac{1}{S}\frac{1}{\beta}\sum_{k}\left(B^{\mu\mu'}_{k-q/2,k+q/2} - B^{\mu\mu'}_{k,k}\right)\Big|_{\omega_q\to 0,\mathbf{q}\to 0} \longrightarrow \sum_{\delta\gamma}\mathcal{T}^{\mu\mu'}_{\delta\gamma}\mathbf{q}_\delta\mathbf{q}_\gamma,
\end{aligned} \tag{S15}$$

where $\mathcal{T}^{\mu\mu'}_{\delta\gamma} = \frac{1}{2}\frac{\partial^2}{\partial\mathbf{q}_\delta\partial\mathbf{q}_\gamma}\left(\frac{1}{S}\frac{1}{\beta}\sum_k B^{\mu\mu'}_{k-\frac{q}{2},k+\frac{q}{2}}\right)\Big|_{\omega_q\to 0,\mathbf{q}\to 0}$. Finally, with inverse Fourier transformation $\phi_\mu(q) = \frac{1}{S}\frac{1}{\sqrt{\beta}}\int d\tau d\mathbf{r} e^{i\omega_m\tau}e^{-i\mathbf{q}\cdot(\mathbf{r}+\tilde{\mathbf{c}}_\mu/2)}\phi_\mu(\tau,\mathbf{r})$ the effective action for the Boson fields in the real space reads

$$S_{\text{eff}}[\overline{\phi},\phi] = \sum_{\mu\mu'}\int_0^\beta d\tau d\mathbf{r}\overline{\phi}_\mu(\mathbf{r},\tau)\mathcal{M}^{\mu\mu'}\phi_{\mu'}(\mathbf{r},\tau) + \sum_{\mu\mu'}\sum_{\delta\gamma}\mathcal{T}^{\mu\mu'}_{\delta\gamma}\int_0^\beta d\tau d\mathbf{r}\partial_\delta\phi^*_\mu(\mathbf{r},\tau)\partial_\gamma\phi_{\mu'}(\mathbf{r},\tau) + O(\phi^4). \tag{S16}$$

The mass term $\mathcal{M}_{\mu\mu'}$ determines the equilibrium configuration via the gap equation $\delta S_{\text{eff}}[\phi,\overline{\phi}]/\delta\overline{\phi} = 0$, while $\mathcal{T}^{\mu\mu'}_{\delta\gamma}$ controls the spatial fluctuation. Without spatial fluctuation and near the transition temperature, the linearization of the gap equation yields an eigenvalue equation $1/(V\Omega)\vec{\Phi} = \boldsymbol{\mathcal{M}}\vec{\Phi}$ [3], where Ω is the area of the moiré unit cell and the matrix $\boldsymbol{\mathcal{M}}$ is given by the components $\mathcal{M}_{\mu\mu'}$. The Eigenvectors $\xi_s = (1,1,1)^T/\sqrt{3}$ and $\xi_{1,2} = \left(1, e^{\pm i\frac{2\pi}{3}}, e^{\pm i\frac{4\pi}{3}}\right)^T/\sqrt{3}$ correspond to extended s-, $(d_{x^2-y^2}+id_{xy})$- and $(d_{x^2-y^2}-id_{xy})$-wave superconductivity, respectively.

II. CALCULATION OF COEFFICIENTS

Here we derive the coefficients $\{\alpha,\beta,\gamma_1,\lambda_1,\lambda_2\}$ used in the main text. The Green function of the free Hamiltonian in the Nambu space $G_0(\omega_m,\mathbf{k}) = \text{diag}\{G_e(\omega_m,\mathbf{k}), G_h(\omega_m,\mathbf{k})\}$, where

$$\begin{aligned}
G^{\pm}_e(\mathbf{k},\omega_m) &= \frac{P_1(\mathbf{k})}{i\omega_m - \varepsilon^{\pm}_1(\mathbf{k})} + \frac{P_2(\mathbf{k})}{i\omega_m - \varepsilon^{\pm}_2(\mathbf{k})},\\
G^{\pm}_h(\mathbf{k},\omega_m) &= \frac{P_1(\mathbf{k})}{i\omega_m + \varepsilon^{\pm}_1(\mathbf{k})} + \frac{P_2(\mathbf{k})}{i\omega_m + \varepsilon^{\pm}_2(\mathbf{k})},
\end{aligned} \tag{S17}$$

are the Green functions in the particle and hole space, respectively. Here,

$$\begin{aligned}
\varepsilon^{\pm}_1(\mathbf{k}) &= t_2(g_{\mathbf{k}} + g_{-\mathbf{k}}) \pm it_3(g_{-\mathbf{k}} - g_{\mathbf{k}}) + t_1|f(\mathbf{k})| - \mu,\\
\varepsilon^{\pm}_2(\mathbf{k}) &= t_2(g_{\mathbf{k}} + g_{-\mathbf{k}}) \pm it_3(g_{-\mathbf{k}} - g_{\mathbf{k}}) - t_1|f(\mathbf{k})| - \mu,
\end{aligned}$$

are the electron and hole dispersions, and

$$P_1(\mathbf{k}) = \frac{1}{2}\begin{pmatrix} 1 & -e^{i\phi_{\mathbf{k}}} \\ -e^{-i\phi_{\mathbf{k}}} & 1 \end{pmatrix}, \quad P_2(\mathbf{k}) = \frac{1}{2}\begin{pmatrix} 1 & e^{i\phi_{\mathbf{k}}} \\ e^{-i\phi_{\mathbf{k}}} & 1 \end{pmatrix} \tag{S18}$$

are the projection operators for these two bands with $e^{i\phi_{\mathbf{k}}} = f_{\mathbf{k}}/|f_{\mathbf{k}}|$. Below we omit the label "±" for simplicity. From Eq. (S15), both the mass and spatial fluctuation depend on

$$\begin{aligned}
\mathcal{B}^{\mu\mu'}_{\mathbf{q},\pm} &\equiv \frac{1}{S}\frac{1}{\beta}\sum_{k} B^{\mu\mu'}_{k-\frac{q}{2},k+\frac{q}{2}} \\
&= \frac{1}{2S}\sum_{\mathbf{k}}\left(\frac{n_F\left(\varepsilon_1(\mathbf{k}-\frac{\mathbf{q}}{2})\right)+n_F(\varepsilon_1\left(\mathbf{k}+\frac{\mathbf{q}}{2}\right))-1}{\varepsilon_1\left(\mathbf{k}-\frac{\mathbf{q}}{2}\right)+\varepsilon_1\left(\mathbf{k}+\frac{\mathbf{q}}{2}\right)}+\frac{n_F\left(\varepsilon_2(\mathbf{k}-\frac{\mathbf{q}}{2})\right)+n_F(\varepsilon_2\left(\mathbf{k}+\frac{\mathbf{q}}{2}\right))-1}{\varepsilon_2\left(\mathbf{k}-\frac{\mathbf{q}}{2}\right)+\varepsilon_2\left(\mathbf{k}+\frac{\mathbf{q}}{2}\right)}\right) \\
&\times\left(\cos\left(\mathbf{k}\cdot(\tilde{\mathbf{c}}_\mu+\tilde{\mathbf{c}}_{\mu'})-\phi_{\mathbf{k}-\frac{\mathbf{q}}{2}}-\phi_{\mathbf{k}+\frac{\mathbf{q}}{2}}\right)+\cos\mathbf{k}\cdot(\tilde{\mathbf{c}}_\mu-\tilde{\mathbf{c}}_{\mu'})\right) \\
&+\frac{1}{2S}\sum_{\mathbf{k}}\left(\frac{n_F\left(\varepsilon_1(\mathbf{k}-\frac{\mathbf{q}}{2})\right)+n_F(\varepsilon_2\left(\mathbf{k}+\frac{\mathbf{q}}{2}\right))-1}{\varepsilon_1\left(\mathbf{k}-\frac{\mathbf{q}}{2}\right)+\varepsilon_2\left(\mathbf{k}+\frac{\mathbf{q}}{2}\right)}+\frac{n_F\left(\varepsilon_2(\mathbf{k}-\frac{\mathbf{q}}{2})\right)+n_F(\varepsilon_1\left(\mathbf{k}+\frac{\mathbf{q}}{2}\right))-1}{\varepsilon_2\left(\mathbf{k}-\frac{\mathbf{q}}{2}\right)+\varepsilon_1\left(\mathbf{k}+\frac{\mathbf{q}}{2}\right)}\right) \\
&\times\left(-\cos\left(\mathbf{k}\cdot(\tilde{\mathbf{c}}_\mu+\tilde{\mathbf{c}}_{\mu'})-\phi_{\mathbf{k}-\frac{\mathbf{q}}{2}}-\phi_{\mathbf{k}+\frac{\mathbf{q}}{2}}\right)+\cos\mathbf{k}\cdot(\tilde{\mathbf{c}}_\mu-\tilde{\mathbf{c}}_{\mu'})\right),
\end{aligned} \tag{S19}$$

which is calculated by the summation over Matsubara frequency. Via Eq. (S19) that is calculated numerically for momentum summation, the coefficients for the mass and spatial fluctuation

$$\begin{aligned}
\mathcal{M}_{\mu\mu'} &= \frac{1}{V\Omega}\delta_{\mu\mu'}+\mathcal{B}^{\mu\mu'}_{\mathbf{q}=0}, \\
\mathcal{T}^{\mu\mu'}_{\delta\gamma} &= \frac{1}{2}\left(\frac{\partial^2}{\partial\mathbf{q}_\delta\partial\mathbf{q}_\gamma}\mathcal{B}^{\mu\mu'}_{\mathbf{q}}\right)\Big|_{\mathbf{q}\to 0},
\end{aligned} \tag{S20}$$

from which we can calculate the coefficients $\{\alpha,\beta,\gamma_1\}$ via their definition in the main text.

Expanding the Bose fields to $O(\phi^4)$, the nonlinear part of the action is given by

$$S^{\mathrm{NL}}_{\mathrm{eff}} = \int_0^\beta d\tau d\mathbf{r}\left(\lambda_1\left(|\psi_1|^2+|\psi_2|^2\right)^2+\lambda_2\left(|\psi_1|^2-|\psi_2|^2\right)^2\right), \tag{S21}$$

in which the coefficients

$$\begin{aligned}
\lambda_1+\lambda_2 &= \frac{1}{2\beta^2}\frac{1}{S}\sum_k \mathrm{tr}\left[G^h_k\Lambda_1(\mathbf{k})G^e_k\Lambda_2(\mathbf{k})G^h_k\Lambda_1(\mathbf{k})G^e_k\Lambda_2(\mathbf{k})\right], \\
\lambda_1-\lambda_2 &= \frac{1}{2\beta^2}\frac{1}{S}\sum_k \mathrm{tr}\left[G^h_k\Lambda_1(\mathbf{k})G^e_k\Lambda_1(\mathbf{k})G^h_k\Lambda_2(\mathbf{k})G^e_k\Lambda_2(\mathbf{k})\right] \\
&\quad+\frac{1}{2\beta^2}\frac{1}{S}\sum_k \mathrm{tr}\left[G^h_k\Lambda_1(\mathbf{k})G^e_k\Lambda_2(\mathbf{k})G^h_k\Lambda_2(\mathbf{k})G^e_k\Lambda_1(\mathbf{k})\right],
\end{aligned} \tag{S22}$$

where

$$\begin{aligned}
\Lambda_1(\mathbf{k}) &= \frac{1}{\sqrt{3}}\begin{pmatrix} 0 & e^{i\mathbf{k}\cdot\tilde{\mathbf{c}}_1}+e^{i\frac{4\pi}{3}}e^{i\mathbf{k}\cdot\tilde{\mathbf{c}}_2}+e^{i\frac{2\pi}{3}}e^{i\mathbf{k}\cdot\tilde{\mathbf{c}}_3} \\ e^{-i\mathbf{k}\cdot\tilde{\mathbf{c}}_1}+e^{i\frac{4\pi}{3}}e^{-i\mathbf{k}\cdot\tilde{\mathbf{c}}_2}+e^{i\frac{2\pi}{3}}e^{-i\mathbf{k}\cdot\tilde{\mathbf{c}}_3} & 0\end{pmatrix}, \\
\Lambda_2(\mathbf{k}) &= \frac{1}{\sqrt{3}}\begin{pmatrix} 0 & e^{i\mathbf{k}\cdot\tilde{\mathbf{c}}_1}+e^{i\frac{2\pi}{3}}e^{i\mathbf{k}\cdot\tilde{\mathbf{c}}_2}+e^{i\frac{4\pi}{3}}e^{i\mathbf{k}\cdot\tilde{\mathbf{c}}_3} \\ e^{-i\mathbf{k}\cdot\tilde{\mathbf{c}}_1}+e^{i\frac{2\pi}{3}}e^{-i\mathbf{k}\cdot\tilde{\mathbf{c}}_2}+e^{i\frac{4\pi}{3}}e^{-i\mathbf{k}\cdot\tilde{\mathbf{c}}_3} & 0\end{pmatrix}.
\end{aligned} \tag{S23}$$

Here we focus on the case with a high hole doping with $\mu \lesssim -t_1$, in which case the particle and hole Green functions $G^h_k \approx \frac{P_2(\mathbf{k})}{i\omega_m+\varepsilon_2(\mathbf{k})}$ and $G^e_k \approx \frac{P_2(\mathbf{k})}{i\omega_m-\varepsilon_2(\mathbf{k})}$, with which, e.g.,

$$\lambda_1+\lambda_2 \simeq \frac{1}{2\beta^2}\frac{1}{S}\sum_{\mathbf{k}}\sum_{\omega_m}\mathrm{tr}\left[\frac{P_2(\mathbf{k})\Lambda_1(\mathbf{k})P_2(\mathbf{k})\Lambda_2(\mathbf{k})P_2(\mathbf{k})\Lambda_1(\mathbf{k})P_2(\mathbf{k})\Lambda_2(\mathbf{k})}{(i\omega_m+\varepsilon_2(\mathbf{k}))^2(i\omega_m-\varepsilon_2(\mathbf{k}))^2}\right].$$

We calculate the summation over Matsubara frequency according to the residue theorem and arrive at

$$\begin{aligned}
\lambda_1+\lambda_2 &= \frac{1}{2\beta}\frac{1}{S}\sum_{\mathbf{k}}\mathrm{tr}\left[P_2(\mathbf{k})\Lambda_1(\mathbf{k})P_2(\mathbf{k})\Lambda_2(\mathbf{k})P_2(\mathbf{k})\Lambda_1(\mathbf{k})P_2(\mathbf{k})\Lambda_2(\mathbf{k})\right] \\
&\quad\times\left[\frac{1}{4\varepsilon_2^2(\mathbf{k})}\Big(n'_F(\varepsilon_2(\mathbf{k}))+n'_F(-\varepsilon_2(\mathbf{k}))\Big)+\frac{1}{4\varepsilon_2^3(\mathbf{k})}\Big(-n_F(\varepsilon_2(\mathbf{k}))+n_F(-\varepsilon_2(\mathbf{k}))\Big)\right],
\end{aligned} \tag{S24}$$

and similarly for $\lambda_1 - \lambda_2$.

---

[1] N. F. Q. Yuan and L. Fu, Phys. Rev. B **98**, 045103 (2018).

[2] M. Sigrist and K. Ueda, Rev. Mod. Phys. **63**, 239 (1991).

[3] A. M. Black-Schaffer and C. Honerkamp, J. Phys. Condens. Matter **26**, 423201 (2014).

[4] M. Claassen, D. M. Kennes, M. Zingl, M. A. Sentef, and A. Rubio, Nat. Phys. **15**, 766 (2019).